

Radiation dose distributions close to the shower axis calculated for high energy electron initiated electromagnetic showers in air

By Stephen Geer and André Gsponer*

Abstract

Absorbed radiation doses produced by 500, 1,000 and 10,000 MeV electron initiated electromagnetic showers in air have been calculated using a Monte Carlo program. The radial distributions of the absorbed dose near to the shower axis are found to be significantly narrower than predicted by simple analytical shower theory. For a 500 MeV, 10 kA, 100 ns electron beam pulse, the region in which the total dose is in excess of 1 krad and the dose rate in excess of 10^{10} rad/s is a cigar-shaped envelope of radius 1 m and length 200 m.

Zusammenfassung

Strahlungsdosen im Bereich der Achsen von hochenergetischen Luftschauern

Mit einem Monte-Carlo-Programm wurden die von elektromagnetischen Luftschauern erzeugten Strahlungsdosen berechnet, die von Elektronen der Energien 500, 1000, und 10 000 MeV ausgelöst werden. Die lateralen Dichteverteilungen der absorbierten Dosen sind in der Nähe der Schauerachse deutlich höher als die einfache analytische Theorie aussagt. Bei Stromstößen mit Elektronen der Energie 500 MeV pro Teilchen von 10 kA Stromstärke und 100 ns Zeitdauer besitzt der Raumbereich, in dem die Gesamtdosis 1 krad und die Dosisleistung 10^{10} rad/s übersteigt, die Gestalt einer langgestreckten Zigarre von 1 m Radius und 200 m Länge.

INIS-EDB-PB-DESCRIPTORS

CASCADE SHOWERS	COSMIC RADIATIONS
ELECTRONS	ACCELERATORS
ELECTROMAGNETIC RADIATION	AIR
RADIATION DOSES	RADIATION DETECTORS
SPATIAL DISTRIBUTION	SHIELDING
SPATIAL DOSE DISTRIBUTION	SHIELDING MATERIALS
MEV RANGE 100-1000	ENERGY TRANSFER
GEV RANGE 01-10	ENERGY LOSSES
MONTE CARLO METHOD	E CODES
POSITRONS	DIRECTED-ENERGY
PHOTONS	WEAPONS

1. Introduction

When a high energy electron passes through air it initiates a cascade of electrons, positrons, and photons: an electromagnetic shower. The radial and longitudinal distributions describing the energy deposition within such showers are of interest to cosmic ray, particle, and accelerator physicists involved in the design of detectors or shielding. Detailed knowledge of these shower distributions near the shower axis is becoming increasingly important with the development of a new generation of high current electron accelerators. Many machines already exist [1] accelerating electrons to energies of a few MeV with currents of 1 kA to 1 MA. Such accelerators are currently in use for laser pumping, flash X-ray radiography, neutron burst production, electron beam fusion experiments, and the simulation of various nuclear weapons effects [2]. This technology is now being extended and the next generation

of high current electron accelerators is expected to produce electron beams of much higher energies. One example is a machine which is being built specifically to investigate the propagation of high intensity electron beams in air, and therefore to determine the feasibility of particle beam weapons. This machine, a 10 kA, 50 MeV electron linac, is under construction in the USA [3] and it has been suggested [4] that machines producing 250 kA pulses of 400 MeV electrons are on the design horizon. The electromagnetic pulse (EMP) effect of beams with currents and energies in this range have already been calculated [4; 5]. The electromagnetic shower calculations presented in this paper provide estimates for the total radiation dose and average radiation dose rate in the immediate vicinity of a high energy electron beam. For targets such as electronic equipment or living tissue, this is important for assessing the lethality of a high energy electron beam weapon.

In this paper the electrons are treated as independent particles. This is true for low current density beams or for single-event applications. For more intense beams, however, the collective behaviour of the electrons within the beam becomes important, the radial profiles are pinched, and the radial spread of the energy deposition presented here should be treated as an upper limit.

In Section 2 of this paper we briefly outline the concepts of simple electromagnetic shower theory, and in Section 3 we discuss the energy deposition in terms of the absorbed radiation dose. We have used a Monte Carlo program to calculate the absorbed radiation doses produced by 500, 1000 and 10000 MeV electron induced electromagnetic showers in air. The details of this Monte Carlo calculation are described in Section 4. Our calculation extends down to radial distances much smaller than the proper scale length for the lateral development of the shower, the so called "Molière length". The results of the calculation are presented in Section 5 and the main results summarized in Section 6.

2. An outline of simple electromagnetic shower theory

The development of an electromagnetic shower involves many complex processes. Several large Monte Carlo programs have been written to facilitate the detailed study of shower development, the particles within the cascade being followed down to very low energies. However, such studies tend to be expensive in terms of computer time, particularly at higher energies where a large number of particles participate in the shower. Fortunately, at these higher energies it is possible to make several simplifications and a number of analytical models [6] have been constructed. The framework and main assumptions of such models are outlined in the following paragraphs. The energy loss of a charged particle passing through matter can be written as:

$$\frac{dE}{dz} = (E + E_c) / X_0 \quad (1)$$

where E/X_0 is the term arising from photon emission by bremsstrahlung in a material of radiation length X_0 , and E_c accounts for the continuous energy loss by ionization. At high energies the energy loss by ionization depends only weakly upon the particles' energy. Therefore, the term E_c is often replaced by a constant, called the "critical energy", which is the ionization energy lost by an electron during its passage through one radiation length of material.

* Dr. Stephen Geer and Dr. André Gsponer, Independent Scientific Research Institute, 9, rue Amat, CH-1202 Genève, Switzerland.

In simple one-dimensional shower theory the lateral development of the shower is neglected and the only photon interaction taken into account is the pair creation process. The primary electron's energy is therefore shared amongst an increasing number of photons, electrons, and positrons whose mean energy decreases as the shower grows. Using such a model, it can be shown that the number of shower particles reaches a maximum at some depth which in the case of the secondary electrons is given by [6]:

$$z_{\max} = X_0 \left(\ln \left(\frac{E_0}{E_c} \right) - 1 \right) \quad (2)$$

where E_0 is the initial energy of the primary electron. In three-dimensional analytical shower theory the lateral spread of the shower must be accounted for. The lateral diffusion due to multiple Coulomb scattering of an electron of energy E passing through a thin layer of material of thickness δz and radiation length X_0 is described by the expression

$$\delta\theta = \frac{E_s}{E} \sqrt{\frac{\delta z}{X_0}} \quad (3)$$

where $E_s = 21.1$ MeV is called the scattering energy, and $\delta\theta$ describes the net deflection of the electron after scattering.

In the two discrete interactions included in simple shower theory, bremsstrahlung emission and pair creation, the angular changes involved are of the order of

$$\delta\theta = \frac{m_e c^2}{E} \quad (4)$$

where m_e and c are the electron rest mass and the velocity of light respectively. By comparing expression (3) with (4) it is evident that for longitudinal distances greater than or of the order of one radiation length the lateral spreading of the shower is dominated by multiple Coulomb scattering of the charged component of the shower. In simple three-dimensional shower theory the lateral spreading of the shower due to the discrete interactions is therefore neglected. One then finds that the particles of highest energy are contained within a core of radius [7]:

$$R_c = \frac{1}{e} X_0 \frac{E_s}{E_c} = \frac{1}{e} X_m \quad (5)$$

where $e = 2.718$ and X_m is called the Molière length. This result can be retrieved if one adopts a very simple model by assuming that the displacement of an electron of energy E is due entirely to multiple Coulomb scattering arising during its passage through the last radiation length of material. Expression (3) then indicates a displacement of the order of $R \approx X_0 E_s / E$. Furthermore at high energies the energy loss is dominated by bremsstrahlung emission and it can be assumed that $E = E_0 \exp(-z/X_0)$. With these assumptions together with expression (2) we obtain Eq. (5).

At the beginning of the shower another estimate of the radial width of the shower distribution is given by the transverse displacement of the primary electron. At high energies the energy loss is dominated by bremsstrahlung emission and the Fokker-Plank diffusion equation describing multiple scattering can be solved in closed form [8].

Averaged over all electron directions, the transverse displacement of the electron is found to be described by a Gaussian distribution with a variance:

$$R_e = \frac{1}{4} X_m \sqrt{\left(\frac{4z^2}{X_0^2} - \frac{2z}{X_0} + 1 \right) \exp\left(\frac{2z}{X_0}\right) - 2} \quad (6)$$

Expressions (5) and (6) are approximate and should be treated only as upper limits to the widths of the radial shower distributions.

3. Energy deposition and radiation dose

As an electromagnetic shower develops the energy of the primary electron is deposited over an extended volume. It is customary to discuss the spatial distribution of the energy deposition in terms of the absorbed radiation dose:

$$D(r, z) = \frac{N}{\rho} \frac{dE}{dV} \quad (7)$$

where dE/dV is the energy deposited per unit volume in a medium of density ρ , and N is the total number of primary electrons. For a single shower $N = 1$, and for a beam pulse of intensity I and duration τ , $N = I\tau/q$ with q equal to the charge of the electron.

In the MKSA system the unit of absorbed radiation dose is the Gray, and $1 \text{ Gy} = 1 \text{ J/kg}$. The traditional unit of absorbed dose is the rad ($1 \text{ rad} = 0.01 \text{ Gy}$). We will express our numerical results in rads.

The main contribution to energy deposition in electromagnetic showers is due to the continuous energy loss of the electrons in the shower by ionization of the medium. To a first approximation one can express (7) in terms of the energy deposited by the ionization process, i.e. $dE/dz \approx E_c/X_0$. In this way we obtain

$$D(r, z) \approx \frac{N}{\rho} \frac{E_c}{X_0} \frac{dP(z, r)}{2\pi r dr} \quad (8)$$

where $dP(z, r)$ is equal to the number of electrons in the shower at the longitudinal co-ordinate z that pass between the radial limits r and $r+dr$. If $dP(z, r)$ has the form

$$\frac{dP(z, r)}{2\pi r dr} = \frac{1}{2\sigma^2} \exp\left(-\frac{r^2}{2\sigma^2}\right) \quad (9)$$

we find that

$$\frac{\int r^2 D(r) dr}{\int D(r) dr} = \frac{1}{2} \frac{\int r^2 dP(r)}{\int dP(r)} \quad (10)$$

Using expressions (5) and (6) we can estimate the widths of the radial dose-distributions at the shower maximum ($z=z_{\max}$) and at the beginning of the shower ($z=X_0$):

$$R(z=z_{\max}) \approx \frac{1}{e\sqrt{2}} X_m \quad (11)$$

$$R(z=X_0) \approx \frac{0.894}{\sqrt{2}} X_m \frac{E_c}{E_0} \quad (12)$$

Finally, one sees that the proper scale factors for the longitudinal-, radial-, and energy-dependence of the electromagnetic shower functions are respectively X_0 , X_m , and E_c . With this in mind it is possible to scale the results presented in this paper for dry air at atmospheric pressure to other media, pressures, or energies.

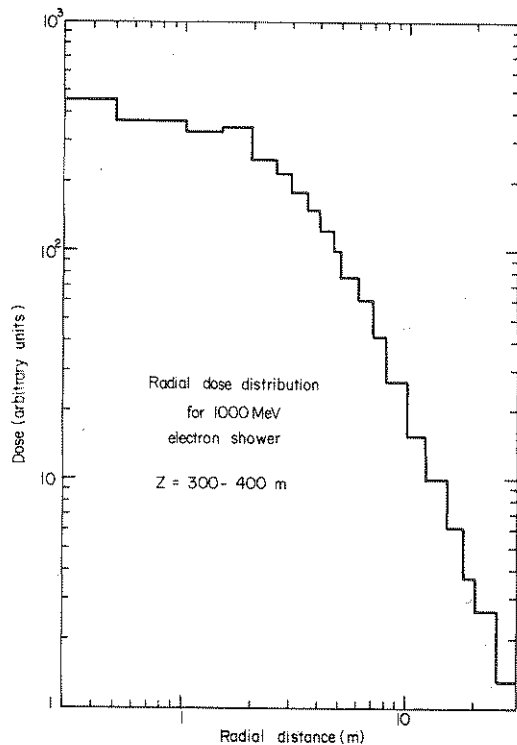


Fig. 1: Histogram of the radial dose distribution between 300 and 400 m for 500 showers induced by 1,000 MeV electrons

4. The Monte Carlo calculation

The electron-gamma shower code EGS [9] was used for the Monte Carlo calculation of the longitudinal- and radial-dose distributions arising from electromagnetic showers initiated by 500, 1,000, and 10,000 MeV electrons in air at atmospheric pressure. The electrons and positrons were followed down to an energy of 1 MeV, and the photons down to 0.1 MeV. Shower particles with less than these cut off energies were assumed to have stopped in the medium and their remaining energy deposited at the position at which they stopped. The shower distributions have been sampled in 20 regions covering the longitudinal shower co-ordinate from 0 to 2,000 m. Each region was therefore 100 m deep. For each of these longitudinal samples the radial dose distributions have been calculated, averaged over the sample. To extract our results these distributions were histogrammed using a binning chosen so that there were at least 5 bins between the shower axis and the radius corresponding to the half maximum of the distribution.

We have generated 500 showers at 500 and 1,000 MeV and 100 showers at 10,000 MeV. To demonstrate the quality of the simulation we present one of the radial dose distributions in Fig. 1 for the 1,000 MeV shower simulation. For convenience in applying our results to problems involving electron beams we present the dose distributions corresponding to 6.25×10^{15} incident electrons. This is equivalent to a 10 kA pulse of duration 100 ns.

5. Results

The energy deposition in air, integrated over the radial shower coordinate, is shown in Fig. 2 as a function of the longitudinal shower depth for electromagnetic showers initiated by a single electron with energies at 500, 1,000 and 10,000 MeV.

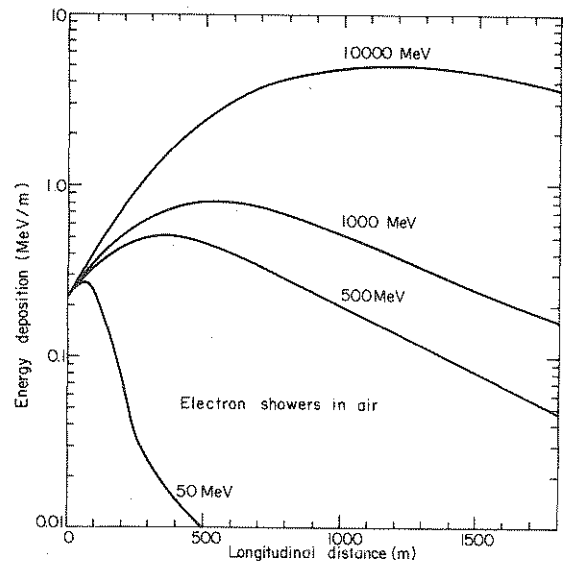


Fig. 2: Laterally integrated energy deposition of showers produced by single primary electrons of various energies as a function of the longitudinal distance

Table 1: Comparison of the radius of the lateral distribution of the absorbed dose at the depth corresponding to the shower maximum estimated by formula (11), R_c , with the result of EGS, $R_{1/2}$

	500 MeV	1000 MeV	10000 MeV
R_c	20 m	20 m	20 m
$R_{1/2}$	~5 m	~5 m	~3 m

Table 2: Comparison of the radius of the lateral distribution of the absorbed dose at the depth $z = X_0$ estimated by formula (12), R_e , with the result of EGS, $R_{1/2}$

	500 MeV	1000 MeV	10000 MeV
R_e	8 m	4 m	0.4 m
$R_{1/2}$	~4 m	~2 m	~0.3 m

In Figs. 3, 4 and 5, for primary electron energies of 500, 1,000 and 10,000 MeV, we present isodose contour plots describing the absorbed dose as a function of the longitudinal and radial shower co-ordinates. The doses have been scaled so that they apply to a 10 kA electron pulse of duration 100 ns. In the same figures the radius $R_{1/2}$ at which the absorbed dose is half of the value on-axis is shown as a broken line. These curves have been replotted on a logarithmic scale in Fig. 6.

The simple shower theory expressions (11) and (12) describing the radial width of the shower at the shower maximum and at one radiation length respectively are compared in Tables 1 and 2 with the EGS results for $R_{1/2}$ at these longitudinal shower co-ordinates. Here we have taken the standard value from Ref. [6] of 81 MeV for E_c . Taking $X_0=301$ m, we have that $X_m=78$ m. The estimate of the radial shower width provided by the simple shower theory expressions are seen to be larger than the estimate provided by the EGS determined value of $R_{1/2}$. In particular the estimate of the shower width at the shower maximum provided by (11) is about a factor of 5 larger than the EGS estimate.

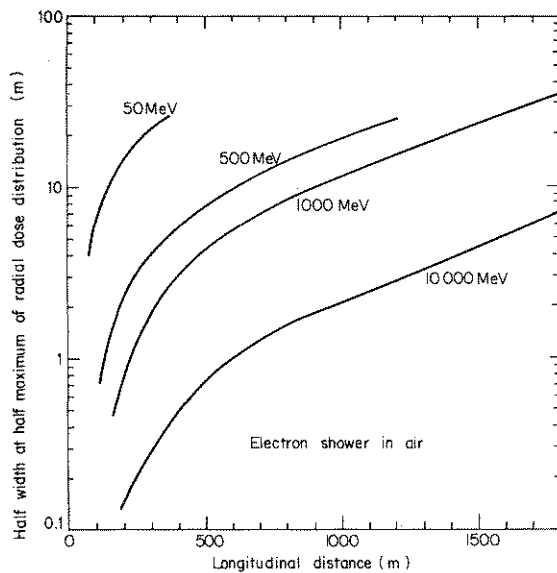
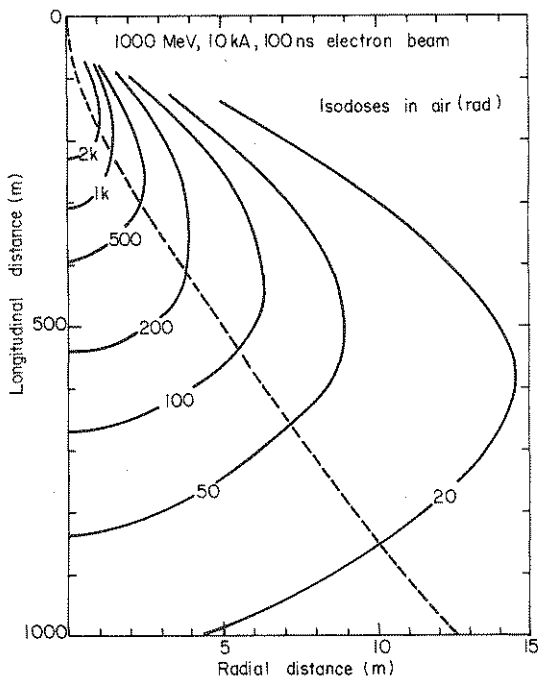
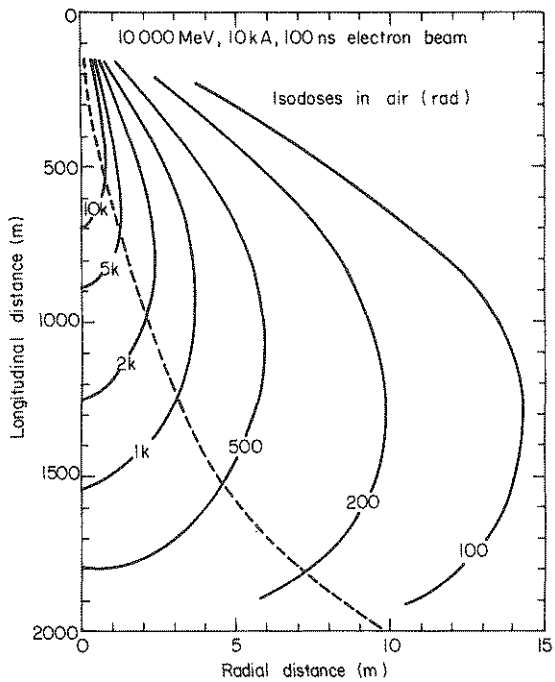
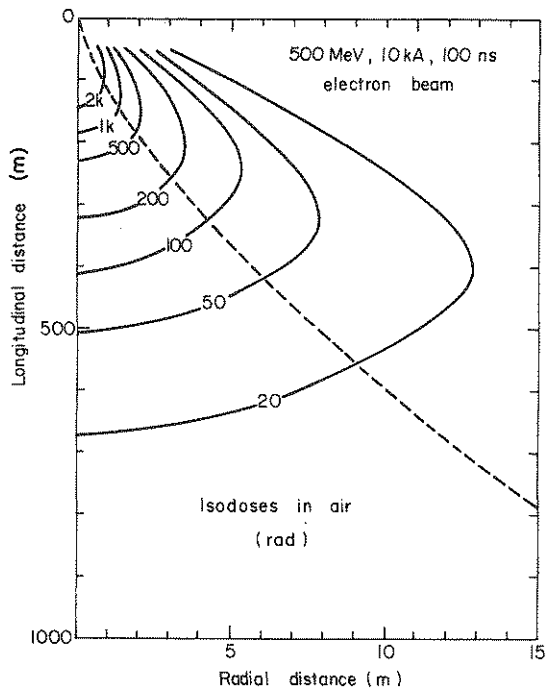


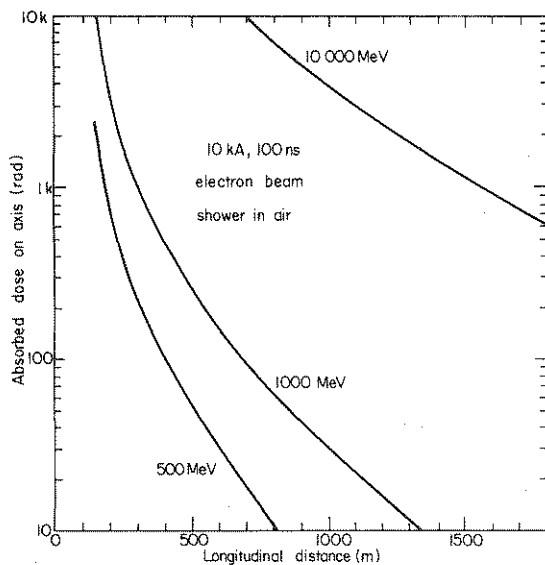
Fig. 3 (top left): Isodose contour plot of the absorbed dose induced by a 500 MeV electron pulse of 10 kA intensity and 100 ns duration

Fig. 4 (center left): Isodose contour plot of the absorbed dose induced by a 1,000 MeV electron pulse of 10 kA intensity and 100 ns duration

Fig. 5 (top right): Isodose contour plot of the absorbed dose induced by a 10,000 MeV electron pulse of 10 kA intensity and 100 ns duration

Fig. 6 (center right): Radius at which the absorbed dose is half the value on the shower axis as a function of the longitudinal distance for various electron energies

Fig. 7 (opposite): Absorbed dose on the shower axis induced by a 10 kA 100 ns electron pulse of various energies as a function of the longitudinal distance



To complete our description of the radiation dose distributions for high energy electron induced electromagnetic showers in air we show the absorbed dose on the shower axis in Fig. 7 as a function of the longitudinal shower co-ordinate. These curves, together with the isodose contours presented in Fig. 3, 4 and 5, provide a detailed picture of the expected absorbed radiation dose as a function of position for showers induced by electrons of energy 500, 1,000 and 10,000 MeV.

6. Summary and application to particle beam weapons

We have used the Monte Carlo code EGS to provide a detailed description of the absorbed dose in air induced by an electromagnetic shower initiated by electrons of energy 500, 1,000 and 10,000 MeV. From this description we extract $R_{1/2}$, an estimate of the shower width, as a function of the longitudinal shower co-ordinate. In comparison with two estimates from simple analytical shower theory, $R(z=z_{max})$ and $R(z=X_0)$, we find that the shower theory estimates are larger than the estimate provided by $R_{1/2}$. We now apply our results to a particle beam weapon, taking for illustration a 500 MeV, 10 kA, 100 ns beam pulse (Fig. 3). An object placed anywhere within a 1 m radius cigar-shaped envelope of length 200 m would be exposed to a radiation dose rate of greater than 1 krad/100 ns = 10^{10} rad/s. This is sufficient to permanently damage any integrated electronic system [10]. For a sequence of beam pulses boring a hole through the atmosphere [11] this envelope could extend over several km in length. For human beings, the lethal dose from radiation sickness is of the order of 500 rad. The use of an electron beam as a radiological weapon is therefore in principle possible. However, in order to reach the 10,000 rad level which is necessary for immediate permanent incapacitation, the beam energy (Fig. 5), current, or pulse duration (or number of beam pulses) should be increased by about an order of magnitude. This seems feasible, provided accelerators producing such beams can be built.

(Received on Febr. 7, 1983; in final form on March 29, 1983)

References

- [1] Keefe, D.: Research on high beam-current accelerators, Particle Accelerators, 11 (1981) 187
- [2] Miller R. B.: An Introduction to the Physics of Intense Charged Particle Beams. 352 pp, Plenum Press, New York 1982
- Gsponer A.: Teilchenbeschleuniger und Fusionstechnologien: Schleichwege zur atomaren Rüstung, Scheidewege, 11 (1981) 552
- [3] Barletta, W. A.: The Advanced Test Accelerator: Generating Intense Electron Beams for Military Applications. Military Electronics/Countermeasures, August 1981, p. 21
- [4] Hobbs, W. E., K. S. Smith: Source-region electromagnetic pulse associated with high-energy electron beams. IEEE Trans. on Nucl. Science, NS-28 (1981) 4451
- [5] Tumolillo T. A., et al.: The radiated electromagnetic field from collimated gamma rays and electron beams in air, IEEE Trans. on Nucl. Science, NS-27 (1980) 1851
- [6] Nishimura, J.: Theory of cascade showers. In Handbuch der Physik, Band XLVI/2, Springer-Verlag, 1967
- [7] Greisen, K.: The extensive air showers. In Progress in cosmic ray physics, III, North-Holland, 1956
- [8] Kazanovskii, M. V., V. E. Pafomov: Solution of the Fokker-Planck equation for a laminar medium. Sov. Phys. JETP, 47 (1978) 442
- [9] Ford R. L., W. R. Nelson: The EGS Code system: Computer programs for the Monte Carlo simulation of electromagnetic cascade showers. SLAC-210, Juni 1978
- [10] Long, D. M.: State-of-the-art review: Hardness of MOS and bipolar integrated circuits. IEEE Trans. on Nucl. Science, NS-27 (1980) 1674
- [11] Winterberg, F.: Electric cloud and weather modification with intense relativistic electron beams. Nature, 247 (1974) p. 271

Induced Mutations – A Tool in Plant Research. Proceedings of a Symposium, Vienna, March 9.–13., 1981. Wien: IAEA 1981. 538 Seiten, zahlreiche Abbildungen, broschiert öS 840.–

Zu diesem interdisziplinär angelegten Symposium kamen 97 Teilnehmer aus 38 Ländern; außerdem waren fünf Organisationen beteiligt. Der hier vorgelegte Bericht ist bis auf einen spanischen und vier französische Beiträge in Englisch abgefaßt und ist dank zahlreicher Abbildungen von ansprechender Aufmachung, auch wenn Satz und Fotodruck kombiniert wurden. Die Grafiken, Schemata, Zeichnungen und Tabellen sind instruktiv, klar konturiert, gut beschriftet und ausreichend groß. Die Qualität der wenigen Schwarzweißfotografien mußte beim gewählten Offsetverfahren natürlich leiden, doch ging das kaum zu Lasten des Informationsgehaltes und der Anschaulichkeit, und die Aufnahmen sind für den Benutzer sehr wertvoll.

Auf 522 Seiten werden in 53 Beiträgen, davon 34 Vorträge und 18 Poster, Forschungsvorhaben vorgestellt, welche mit Hilfe von Induktionsmutanten unterschiedlichsten Fragen der Pflanzenzüchtung und Pflanzenproduktion nachgehen. Neben der klassischen Genforschung stehen angewandte Untersuchungsziele wie Ertragssteigerung oder Vereinfachung der Erntetechniken im Vordergrund.

Dem Symposiumsablauf entsprechend ist der Band in acht Abschnitte gegliedert. Einem Übersichtsreferat folgen jeweils Einzelversuchsberichte. Literaturangaben und Auszüge aus den Diskussionen heben den Informationswert dieser Abhandlungen. Von den Postern sind kurze Textfassungen abgedruckt.

Das erste Kapitel befaßt sich mit der Rolle der Induktionsmutanten für den Fortschritt der Genetik, wobei Theorie wie auch Praxis berücksichtigt werden. Während hier meistens von Getreidearten die Rede ist, behandelt das nachfolgende Kapitel die Evolution verschiedenster, auch gärtnerischer Kulturpflanzen. Im sich anschließenden Abschnitt über pflanzenphysiologische Untersuchungen steht die Verbesserung des Erntegutes, seien es die Biomasse oder Einzelkomponenten wie Eiweißertrag oder biochemische Merkmale, im Blickpunkt des Interesses. Dem heute besonders beachteten Verhalten von Pflanzenschädigern und der Gewinnung resistenter Pflanzenarten über die Induktion von Mutanten widmet sich das vierte Kapitel. Auch das Kapitel über Pflanzensymbiosen, vorwiegend unter Beteiligung von N-Bakterien, beschäftigt sich mit einem ökologisch wie ökonomisch sehr aktuellen Problem. Demgegenüber stellt der sechste Abschnitt, Induktionsmutanten und in-vitro-Kultur, eher theoretische und gentechnische Fragen, untersucht an Zier- wie auch an Nutzpflanzen, in den Vordergrund. Genökologie war das Thema einer siebten Symposiumssitzung; Blütezeit und Kältetoleranz seien als Stichworte genannt. Ausgesprochen angewandt ist die Thematik des achten Kapitels: Induktionsmutanten und Pflanzenzüchtung; hier reicht der Bogen von der genetischen Analyse über Mutationsprozesse bis zur Mutagenese in heranwachsenden Pflanzen. Zum Abschluß sind Vorschläge für künftige, sehr wünschenswerte Forschungsarbeiten über Erbeigenschaften, die nicht auf der Kern-DNS lokalisiert sind, zusammengefaßt.

Was diesen Band auszeichnet und dadurch empfehlenswert nicht nur für Evolutionsgenetiker, sondern für die Vertreter verschiedenster pflanzenbaulicher Disziplinen macht, ist neben der klar gegliederten, breiten Spanne von Arbeitsrichtungen die Vielfalt von Pflanzen, die außer klassischen Untersuchungsobjekten wie Nicotiana die verschiedensten Getreidearten, mono- und dikotylen Futterpflanzen, zahlreiche Gemüsearten und eine Reihe von Zierpflanzen umfaßt. Naturgemäß sind krautige Gewächse mit kurzer Generationsphase erklärte Versuchsobjekte der Genetiker, doch findet sich auch ein Beitrag über Kirsche, Thuja und – neuerdings interessant – Kenaf. Beitragsfülle und Pflanzenvielfalt verweisen gleichermaßen darauf, daß allgemeingültige Aussagen auf der Basis induzierter Mutationen unzulässig sind. Angesichts des Pflanzensortiments wäre deshalb neben dem Autorenverzeichnis und der nach Ländern geordneten Teilnehmerliste sowie der SI-Einheiten-Umrechnungstabelle ein Artenindex wünschenswert und bei dem Buchpreis eigentlich zu erwarten. Der Wert des Buches als Nachschlagewerk würde dadurch erhöht.

Insgesamt gesehen legt die IAEA hier einen aufschlußreichen Sammelband vor, der zusätzlich zur Gentechnologie neuere Entwicklungen bei landwirtschaftlichen und gärtnerischen Nutzpflanzen aufzeigt. Inhalt und Aufmachung bieten dem einschlägig Forschenden und dem Lehrenden Information, Anregung oder gar Unterrichtshilfe.

U. Hornung, Norath